Capillarity Driven Instability of a Soft Solid

Serge Mora,[*] Ty Phou, and Jean-Marc Fromental

Laboratoire des Colloïdes, Verres et Nanomatériaux, UMR 5587, Université Montpellier 2 and CNRS,
Place Eugène Bataillon, F-34095 Montpellier Cedex, France

Len M. Pismen

Department of Chemical Engineering and Minerva Center for Nonlinear Physics of Complex Systems,
Technion—Israel Institute of Technology, Haifa 32000, Israel

Yves Pomeau

Department of Mathematics, University of Arizona, Tucson, Arizona, USA

We report the observation of a Plateau instability in a thin filament of solid gel with a very small elastic modulus. A longitudinal undulation of the surface of the cylinder reduces its area thereby triggering capillary instability, but is counterbalanced by elastic forces following the deformation. This competition leads to a nontrivial instability threshold for a solid cylinder. The ratio of surface tension to elastic modulus defines a characteristic length scale. The onset of linear instability is when the radius of the cylinder is one-sixth of this length scale, in agreement with theory presented here.

The Rayleigh-Plateau instability (RPI) [1–4] results from the tendency of a given volume of liquid to reduce its area at constant volume. The area of a geometrical cylinder is obviously not at a minimum, this one being reached, as is well known, for a sphere. A long-wave modulation of the surface of a cylinder is unstable: near the maxima of the radius, the Laplace pressure, which is dominated by the azimuthal curvature, decreases and pushes the fluid outward, the converse being true for the minima of the radius where the increase of the Laplace pressure pushes the fluid inward.

Although surface tension exists in solids as well, its effect on the pattern formation is believed to be unobservable at macroscopic scale because surface energy is negligible compared to elastic energy of deformation. Perhaps the only phenomenon where surface tension plays a role is crystal faceting [5] where it does not compete with elastic forces. The RPI may be, however, relevant in soft solids, such as those found very often in biology, and so may play a role in such biological processes as generation of filaments, formation of beaded forms in myelinated nerve fibers, etc. It also provides a unique method for fabricating undulating cylinders with a wavelength controlled by physical parameters. Such cylinders with undulation period in the range of optical wavelength could show, for instance, forbidden wave bands for the propagation of light.

In solids, contrary to liquids, the energy has a volume part that changes alongside modulation of the external surface. As is often noticed, the balance between the two kinds of energies, capillary and elastic, depends on a quantity with the dimension of length $l = \gamma/\mu$, where γ is surface tension and μ is the elastic shear modulus. In usual solids, this is a very small length scale: because of its origin in atomic interactions, one expects l to be of the order of the range of atomic interactions, about a fraction of a nanometer. Therefore the capillary effect, in the numerator of the small length scale, should be typically negligible. Nevertheless, in a very soft solid like a gel just above the percolation threshold, this length scale can be macroscopic. The reason is that the complex molecular structure of such materials reduces by many orders of magnitude the "typical" value of the shear modulus computed from the standard molecular parameters, such as the size of an atom and the energy of a covalent bond. Measured values for γ are few tens of mN/m and for μ measured values are few tens of Pa (very small by comparison with ordinary materials); therefore, l, as well as the expected typical length scale for elastic RPI, may go up to the millimeter range, well above any microscopic length scale of this kind of material.

To demonstrate RPI in a solid, we have used a standard agar gel (Merck KGaA, Germany) dissolved in purified water. Small amounts of methylene blue were added to agar solutions to aid observations. Agar is known to dissolve in boiling water and to form a gel upon cooling to about 35 °C [6,7]. Upon cooling, the shear modulus first rapidly increases and then stabilizes (Fig. 1). A cooled gel behaves as an incompressible elastic solid over a wide frequency range (at least from 300 to 10^{-3} Hz; Fig. 1). We have carefully checked rheological properties of agar gels and measured the shear modulus at various concentrations (from 0.5% to 0.16%).

The experiments are carried out as follows. Liquid solutions of agar (90 °C) with various concentrations are first
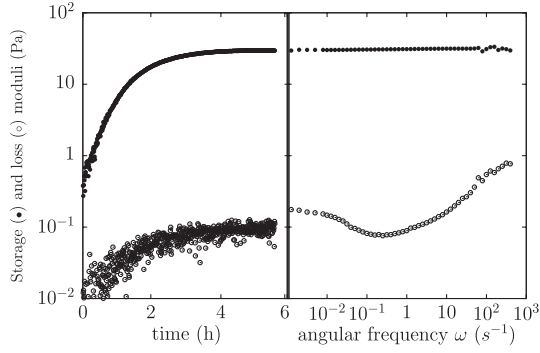
FIG. 1. Linear rheological properties of a 0.18% agar gel hydrogel. The curves are obtained by dynamic oscillatory shear tests, using a strain controlled rheometer (ARES-RFS from TAInstruments) in Couette geometry. Left: Evolution of the storage and loss moduli as functions of time. Right: Storage and loss moduli as functions of the angular frequency 5 h after cooling.

injected in cylindrical moulds made of cellular polystyrene. These moulds are fabricated using two cuboid pieces of cellular polystyrene ($3 \times 0.5 \times 0.5$ cm^3). One of the larger faces of each piece is heated just above the glass transition temperature of polystyrene. The two hot sides are then assembled and a 3 cm long copper wire of a desired diameter is inserted between them. This wire is removed after cooling at room temperature, leaving a hollow cylinder of the same dimensions within the polystyrene block. We have checked by optical microscopy that the roughness of the surface is less than 4 μm. The mould is then pre-heated in order to prevent partial gelation before the liquid is completely injected.

After injecting the agar solution and cooling for 5 h at room temperature, the mould is dissolved in liquid toluene. Total dissolution takes about 3 min. The strand of agar gel is then released in toluene. The agar gel—toluene surface tension γ is roughly equal to the water-toluene surface tension; this value is used in further computations. To prevent the agar cylinder from wrapping up, the two ends are fixed in a frame before releasing. This yields strands measuring about 2 cm long floating in toluene. Depending on the mould, their radius lies in the range 150–260 μm.

Depending on the initial strand radius ρ_0 and the shear modulus μ of the agar gel, the growth of a surface instability takes place during the mould dissolution. The final steady pattern is seen after dissolution is complete. Strands of agar gel with a high concentration and/or a large radius retain a cylindrical shape after the mould dissolution [Fig. 2 (a)]. Strands with a low concentration and a small radius are systematically breaking into two during the dissolution. For intermediate strands, surface undulations develop just after dissolution and remain permanently [Figs. 2(b)–2(d)]. When an unstable filament is gently stretched in the middle, and then released, it recovers its length and shape, thereby demonstrating that the undulation pattern is stable. On the contrary, if pure water is injected into the moulds instead of
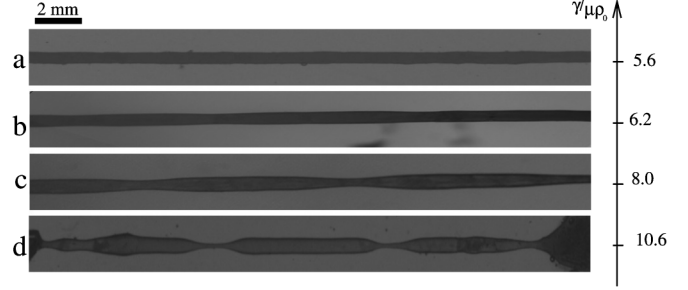
FIG. 2. Equilibrium shape of agar gel cylinders for different values of the shear modulus. Radius is $\rho = 240$ μm, surface tension is $\gamma \simeq 36.5$ mN/m. Shear modulus varies from 12 to 27 Pa. Note the RPI instability for values of $\gamma/(\mu\rho)$ larger than 6.2.

the agar gel, the released strand breaks, as expected, into separate spherical droplets.

We used toluene saturated with water to prevent shrinking. This makes a fundamental difference between our experiments and those reported by Matsuo and Tanaka [8]. In their case, the instability is driven by diffusion of the gel solvent into the miscible outer fluid. The slowly developing instability they observe cannot be linked to a RPI, because there is no sharp interface and so no surface tension in their experiment.

Within the setup we used, the resolution for the amplitude of the modulations is about 15 μm. To obtain the critical elastic modulus (at a fixed radius) below which cylinders remain straight, the amplitude is plotted as a function of the elastic modulus and fitted by the power law

$$f(\mu) = \alpha(\mu - \mu_c)^\beta \qquad (1)$$

with adjustable parameters α, β, and μ_c (Fig. 3); μ_c is the shear modulus at the instability threshold. In this way, we succeed in separating unambiguously the cases where a cylinder is either stable or not. Figure 4 summarizes the experimental stability data in the $\mu - \rho_0$ plane. The plane is divided into two areas, one corresponding to stable straight cylinders and the other to unstable ones.

Just above the threshold [Fig. 2(b)], the instability leads to a varicose shape. Farther away from the threshold, the shape becomes more complicated, with large constant-radius areas interrupted by constrictions [Fig. 2(d)]. In the following, we focus on the physics near the threshold [Figs. 2(a) and 2(b)]. The analysis far beyond the instability threshold requires a nonlinear theory that will be the subject of future work.

Suppose that the surface of a cylinder is perturbed by a small axisymmetric modulation from a constant radius ρ_0 to $\rho(z) = \rho_0 + \lambda(z)$, where z is the coordinate along the axis and $\lambda(z) \ll \rho_0$ (Fig. 5). The mean curvature κ of the surface changes from $1/\rho_0$ to $1/\rho_0 - \lambda(z)/\rho_0^2 - \lambda''(z)$. This yields a Laplace pressure contribution $\gamma\kappa$ to be added to the boundary conditions (bc) for the normal stress on the surface of the cylinder.
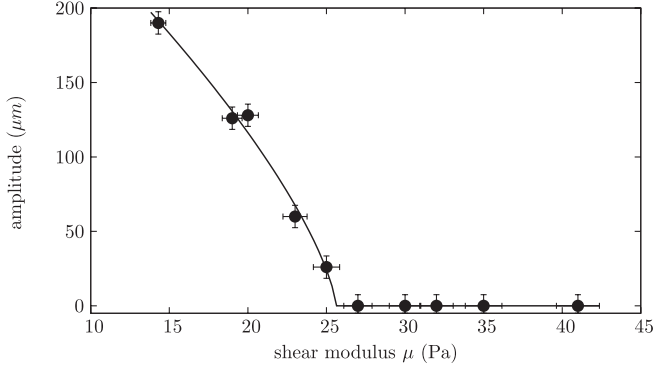
FIG. 3.   The modulation amplitude as a function of the shear modulus for a fixed radius of the strands ($\rho = 240$ μm). The solid line is the best fit according to Eq. (1) with $\mu_c = 25.6$ Pa, $\alpha = 34.1$ μm, and $\beta = 0.71$.

Our material can be considered as incompressible, so that its only relevant Lamé coefficient is the shear modulus μ. Using a variational formulation, we write the elastic energy in the cylindrical coordinates r, z as

$$\mathcal{E} = 2\pi \int dz \int_0^\rho dr r \Big[\mu \Big(u_{r,r}^2 + u_{z,z}^2 + \frac{u_r^2}{r^2} + \frac{1}{2}(u_{r,z} + u_{z,r})^2 \Big) - p \Big(u_{r,r} + \frac{u_r}{r} + u_{z,z} \Big) \Big], \tag{2}$$

where u_r, u_z are the radial and axial displacements, the indices preceded by a comma denote respective partial derivatives, and p is the Lagrange multiplier imposing the incompressibility condition

$$u_{r,r} + \frac{u_r}{r} + u_{z,z} = 0. \tag{3}$$

By variation with respect to the displacements u_r and u_z, one gets the Cauchy-Poisson equations in cylindrical coordinates:
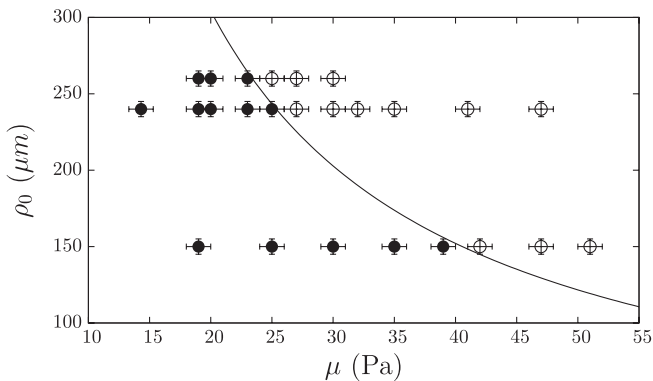
FIG. 4.   A series of agar cylinders with different shear modulus has been investigated for each radius. The empty symbols correspond to stable cylinders and filled symbols to unstable cylinders acquiring a varicose shape. The parametric plane $\rho_0 - \mu$ is separated into two domains by the theoretical curve $\gamma/(\mu \rho_0) = 6$ (without fitting parameters) derived in this Letter.

$$\mu[2u_{z,zz} + (u_{r,z} + u_{z,r})_{,r} + r^{-1}(u_{r,z} + u_{z,r})] - p_{,z} = 0, \tag{4}$$

$$\mu(u_{r,zz} - u_{z,zr}) - p_{,r} = 0. \tag{5}$$

The latter equation has been rearranged using the incompressibility condition (3) and the identity

$$u_{r,rr} + \frac{u_{r,r}}{r} - \frac{u_r}{r^2} = \Big(u_{r,r} + \frac{u_r}{r} \Big)_{,r}.$$

The two boundary conditions on the free surface $r = \rho(z)$ express the continuity of stress (including the Laplace capillary pressure), supplemented by two conditions of smoothness at $r = 0$. The Laplace pressure comes from the variation of the capillary energy equal to the area of the perturbed cylinder times surface tension γ. Assuming cylindrical symmetry, this energy reads

$$\mathcal{A} = 2\pi \gamma \int \rho(z)\sqrt{1 + \rho_{,z}^2} dz.$$

The variation of the capillary energy caused by changing the shape of the surface of the cylinder reads

$$\delta \mathcal{A} = 2\pi \int \delta\rho(z) \Big(\sqrt{1 + \rho_{,z}^2} - \frac{\rho_{,zz}\rho(z)}{(1 + \rho_{,z}^2)^{3/2}} \Big) dz.$$

This expression has to be added to the contribution $\delta\mathcal{E}_b$ to the variation of $\mathcal{E}$, which comes from the boundary term after integration by parts:

$$\delta\mathcal{E}_b = 2\pi \int \rho(z)[\delta u_r(2\mu u_{r,r} - p) + \mu \delta u_z(u_{r,z} + u_{z,r})]dz,$$

where the integrand is evaluated at $r = \rho(z)$.

Writing now that $\delta\rho(z) = \delta u_r$ at $r = \rho(z)$, and requiring $(\delta\mathcal{E}_b + \delta\mathcal{A})$ to vanish for any possible δu_r and δu_z, one finds the following bc for the tangential and normal stress on the surface:

$$u_{r,z} + u_{z,r} = 0, \tag{6}$$

$$-\gamma\Big(\frac{u_r}{\rho_0^2} + u_{r,zz} \Big) + 2\mu u_{r,r} - p = 0. \tag{7}$$
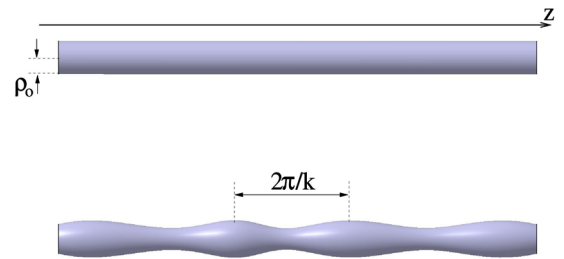
FIG. 5 (color online).   Sketch of a straight cylinder before and after a varicose perturbation. The energy increment may be of either sign, depending on the radius, the surface tension, and the shear modulus.

In the last condition, the uniform equilibrium pressure inside the unperturbed straight cylinder given by the standard Laplace value, γ/ρ_0, has been subtracted from p. The problem of linear stability amounts to finding a nontrivial solution of Eqs. (4), (5), and (3) with the bc (6) and (7), imposed at $r = \rho_0$.

In a standard way, we assume a harmonic z dependence of any physical quantity of the order of the perturbation $\sim e^{ikz}$ with a wave number k. Then one can express from Eq. (4) $p(r, k)$ as a function of $v = u_r$ and its derivatives, and use the result in (5) to get a fourth-order equation for v:

$$(\mathcal{L} - k^2)^2 v = 0, \qquad \mathcal{L} = \frac{d^2}{dr^2} + \frac{1}{r}\frac{d}{dr} - \frac{1}{r^2}. \qquad (8)$$

Omitting terms diverging at $r = 0$, the general solution of Eq. (8) is found by using the Wronskian method and can be presented as

$$v(r) = \alpha I_1(kr) + \beta k^2 \left[K_1(kr) \int_r^\rho I_1^2(kr')r'dr' - I_1(kr) \right.$$
$$\left. \times \int_r^\rho r' I_1(kr')K_1(kr')dr' \right], \qquad (9)$$

where I_a and K_a are the modified Bessel function of first and second kind of order a, respectively, and α and β are integration constants. Using Eqs. (3)–(5), the bc (6) and (7) at $r = \rho$ can be expressed in terms of v and its derivatives.

These bc involve the third derivative of v at most, consistent with the fact that Eq. (8) is of the fourth order. Functions singular at $r = 0$ have been excluded by the particular choice of solution in Eq. (9). Using the general solution given by Eq. (9) in the bc (6) evaluated at $r = \rho_0$ and taking note that the integrals in (9) vanish at this point yields $\beta = 2\alpha$. Upon this substitution, we find from the bc (7) that the nontrivial solution exists at the critical value

$$\gamma_c = \frac{2\mu\rho_0}{1 - \rho_0^2 k^2}\left[\frac{2k\rho_0 I_0(k\rho_0)}{I_1(k\rho_0)} - 1 \right]. \qquad (10)$$

Instability occurs at $\gamma > \gamma_c$. It first appears in the long-scale mode $k \to 0$ at $\gamma_c(0) = 6\mu\rho_0$. The instability limit diverges at $k \to 1/\rho_0$.

The curve representing the equation $\gamma = 6\mu\rho_0$ is plotted in the $\mu - \rho_0$ plane in Fig. 4. The toluene-agar gel surface tension is taken as the measured value $\gamma = 36.5$ mN/m. This curve, directly following from the theory with no adjustable parameters, well matches the boundary between the two domains (for stable or unstable cylinders) detected experimentally. The finite wavelength observed in experiments may be either an indication of a slight subcriticality of the instability or a manifestation of nonlinear effects, necessarily present when the instability is observed at the macroscopic scale.

This above exact result for γ_c has been viewed as an approximation by Barrière *et al.* [9] who have used this

approach to explain pattern formations during shrinkage of polymer gels reported by Matsuo and Tanaka [8]. In these experiments, the swollen gel in the cylinder becomes surrounded by a shrunken skin of macroscopic thickness. Assuming that the skin acts as an effective surface tension, Barrière *et al.* have found that the orders of magnitude might be in the right range to explain surface instability observed by Tanaka and Matsuo [9]. In these experiments the instability was, however, driven by a skin action modeled by a surface tension rather than by capillarity. Inferring surface tension out of a macroscopic concentration gradient may be problematic: according to the Kirkwood-Buff formula [10], surface tension requires an anisotropic stress tensor in the transition region. Such an anisotropy certainly exists near the interface between the water of our gel and toluene because of their immiscibility, but does not *a priori* exist for two miscible phases, like those of Tanaka and Matsuo. The main distinctive features of our experiments are (i) far smaller elastic moduli of agar gels and (ii) absence of a macroscopic skin at the agar gel surface. The last point is particularly important, and the good agreement between theory and our experiments for the onset value is a strong argument in favor of capillary effects as the cause of the observed instability.

In conclusion, we have given experimental evidence of Rayleigh-Plateau instability in a cylinder of soft solids. Its onset is well described by theory. Contrary to the RPI in liquids, the instability evolves to a steady wavy pattern along the cylinder. From the experiments we conjecture that, beyond a second critical (nonlinear) threshold, the final state is a set of disconnected droplets of solid, like in the case of a fluid cylinder.

*smora@univ-montp2.fr

[1] J. Plateau, *Statique Expérimentale et Théorique des Liquides Soumis aux Seules Forces Moléculaires* (Gauthier Villars, Paris, 1873), Vol. II.
[2] Lord Rayleigh, Proc. London Math. Soc. **s1-10**, 4 (1878).
[3] Lord Rayleigh, Proc. R. Soc. London **29**, 71 (1879).
[4] J. Eggers, Rev. Mod. Phys. **69**, 865 (1997).
[5] L. Landau and E. Lifschits, *Statistical Physics* (Pergamon, Oxford, 1980), 3rd ed., Chap. 155, pp. 520–523.
[6] N. Stanley, *Agar* (CRC Press, Boca Raton, FL, 2006), 2nd ed., Chap. 7, pp. 217–231.
[7] R. Lapasin and S. Pricl, *Rheology of Industrial Polysaccharides: Theory and Applications* (Blackie Academic Professional, Glasgow, 1995).
[8] E. Matsuo and T. Tanaka, Nature (London) **358**, 482 (1992).
[9] B. Barrière, K. Sekimoto, and L. Leibler, J. Chem. Phys. **105**, 1735 (1996).
[10] J. Kirkwood and F. Buff, J. Chem. Phys. **17**, 338 (1949).